Influence of Bed Depth on Specific Liquid-Solid Mass Transfer in a 5 m Trickle Bed Reactor

Francois Saayman

Influence of Bed Depth on Specific Liquid-Solid Mass Transfer in a 5 m Trickle Bed Reactor

Francois Saayman

Submitted in the partial fulfilment of the requirements for the degree Masters in Engineering (Chemical Engineering) in the Faculty of Engineering, Built Environment and Information Technology, University of Pretoria, Pretoria.

24 April 2014

Influence of Bed Depth on Specific Liquid-Solid Mass Transfer in a 5 m Trickle Bed Reactor

by

Francois Saayman

Promoter: Professor Willie Nicol

Department of Chemical Engineering

Masters in Engineering (Chemical Engineering)

Synopsis

Trickle bed reactors (TBRs) exhibit complex hydrodynamics and this study is aimed at giving insight into whether liquid-solid mass transfer and wetting are influenced by bed depth in a 5 m trickling column using 4 mm glass spheres as random packing. Measurements were made using the novel electrochemical technique developed by Joubert and Nicol (2013). Using this technique the wetting and mass transfer could be measured simultaneously.

The study proves that the liquid-solid mass transfer and wetting efficiency do not stabilise at a minimum bed depth. The parameters were found to continue decreasing until the bottom of the bed. For the upper branch of the hydrodynamic envelope, the rate of decrease for the wetting efficiency was slow at the top of the bed and decreased rapidly closer to the bottom. However, only the wetting efficiency decreased significantly as a function of bed length; the liquid-solid mass transfer exhibited only a slight decrease of 14%. This compared well with the results of Du Toit *et al.* (2014), who found an 11% decrease in the liquid-solid mass transfer in a column with an x/D value of 29,4. The lower branch of the hydrodynamic envelope showed a linear decrease with respect to bed length for both wetting and mass transfer. The liquid-solid mass transfer decreased by 50% from the top of the bed to the bottom. These results are also in agreement with those of Du Toit *et al.* (2014)[1] who found a decrease of 30% for a 1,6 m column. The wetting efficiency for the

[1] Du Toit *et al.* (2014): This refers only to the data in the short column in the article, whereas the results of the current study were used for the longer column.

Levec mode decreased by 52%, whereas Du Toit *et al.* (2014)[2] found a decrease of 20%.

Keywords: Liquid-solid mass transfer; Wetting efficiency; Liquid-solid contact; Electrochemical measurement

[2] Du Toit *et al.* (2014): This refers only to the data in the short column in the article, whereas the results of the current study were used for the longer column.

Contents

List of figures

List of tables

Nomenclature

N	Reaction rate per unit area	
T	Transfer number	
I	Current	A
C	Concentration	kmol/m^3
k	Mass transfer coefficient	m/s
A	Column area	m^2
ρ	Density	kg/m^2
f	Wetting fraction (The fraction of the total external area of the particles that is wetted with liquid)	
D	Column diameter	m
F	Faraday constant	C/mol
d_p	Particle diameter	mm

Subscripts

L	Liquid
LS	Liquid-solid
B	Bulk
W	Surface

1. Introduction

Fixed-bed reactors that process both liquid and gas streams are the most commonly used reactors in the petrochemical and chemical industries. These reactors can be operated either in co-current downflow or counter-current flow. Fixed beds with co-current downflow are known as trickle bed reactors (TBRs). Traditionally, TBRs are used in the refinery industry for the hydro-treatment of hydrocarbon streams, such as hydrocracking and desulphurisation of process streams (Al-Dahhan *et al.*, 1995). Trickle bed reactors are ideally suited to processing large streams. This is due to the flexibility in the throughput of the liquid and gas to the reactor. At low throughput the trickle flow regime occurs, which has complex hydrodynamics. This has a significant effect on the overall performance of the reactor. In order to model a reactor properly, in-depth knowledge is required of both the hydrodynamics of the bed and the kinetics of the catalyst.

There have been numerous studies aimed at quantifying the effect that hydrodynamics have on the overall reactor performance. Several correlations have been proposed (Duduković *et al.*, 2002; Al-Dahhan *et al.*, 1995). Only a few of these studies aimed to quantify the effect that reactor depth has on the hydrodynamics (Reis, 1967; Dutkai & Ruckenstein, 1968; Gostick, 2003; Baussaron *et al.*, 2007a,b & c; Shubert *et al.*, 2008; Du Toit *et al.*, 2014). Two clear theories have emerged in the open literature; one school of thought is that the hydrodynamics stabilise within the first few centimetres of the reactor (Gostick, 2003; Baussaron *et al.*, 2007a,b & c; Shubert *et al.*, 2008), while other studies have shown that the hydrodynamics do not stabilise at all (Nicol & Joubert, 2013; Joubert & Nicol, 2013; Du Toit *et al.*, 2014*).

Two of the prominent hydrodynamic properties that have a direct influence on the reactor performance for liquid-limited reactions are the liquid-solid mass transfer (LSMT) and the wetting efficiency. A dimensionless column length (x/D) is used to compare studies. This normalised depth required for stabilisation varies from study to study. However, the general consensus is that increased drip point density decreases the x/D value required for stabilisation. The study by Dutkai and Ruckenstein (1968) used a point source distributor and found stabilisation at an x/D of 9.7, whereas the studies by Baussaron *et al.* (2007a, b & c) used a multipoint

distributor with a drip point density larger than 18 000 drips/m^2 and found stabilisation at an x/D value of 0.5 – this was for porous particles. Du Toit *et al.* (2014)*, however, found that even after a bed depth of x/D = 23.5 (1.6 m) the wetting and liquid-solid mass transfer did not stabilise – this was for solid particles.

This study was aimed at investigating whether the liquid-solid mass transfer and external wetting efficiency stabilise in a deep bed (5 m), by using the novel electrochemical technique of Joubert and Nicol (2013). A 5 m trickling column with an internal diameter of 105.6 mm was used; this length resulted in an x/D value of 47. The bed was packed with 4 mm glass beads and sections of 4.5 mm nickel-coated steel beads to serve as the electrodes. With this new novel electrochemical method both the external wetting efficiency and the liquid-solid mass transfer coefficient can be measured simultaneously.

2. Literature review

2.1. *Trickle bed hydrodynamics*

Trickle-bed reactors are fixed-bed three-phase reactors with co-current downflow of liquid and gas over a stationary bed of catalyst particles. Among three-phase reactors trickle-bed reactors are the most widely used (Al-Dahhan *et al.,* 1995; Al-Dahhan & Duduković, 1995). They are used in the petroleum, petrochemical, biochemical and chemical industries, as well as the waste water sector. From an economic point of view, the optimal operation of these reactors is very important since the products processed by TRBs annually are estimated to reach 1,6 billion metric tons (Al-Dahhan *et al.,* 1995). TRBs exhibit complex hydrodynamics due to their three-phase nature. This results in two clear regimes within which a TBR can be operated, namely the low-interaction regime (LIR) and the high-interaction regime (HIR). The low-interaction regime is commonly referred to as the *trickle flow regime*. The high-interaction regime can be divided into three subregimes: the *bubble, pulsing and spray flow*. This study is focused on the low-interaction regime.

Since the fluid structures surrounding a particle are so complex in the trickle flow regime, hydrodynamic parameters cannot be derived fundamentally and are normally correlated (Al-Dahhan & Duduković, 1995). The correlations are typically performed by using parameters such as hold-up, pressure drop and liquid velocity (Duduković *et al*., 2002). A prominent correlation is the Larachi calculator (Larachi & Grandjean, 1999) which is a neural network estimator of all the published data and correlations up until the late 1990s. In the review paper by Duduković *et al.* (2002) an extensive compilation of TBR correlations can be found for each hydrodynamic parameter. A comprehensive study on the hydrodynamic effects in a trickle bed reactor is presented in this section.

2.2. *Hydrodynamic multiplicity and flow structures of trickle flow*

In the trickling regime or the low-interaction regime (LIR) the liquid flow structures may differ from one bed to the next, even if the two beds are running at the same superficial liquid and gas velocities. This phenomenon is called *hydrodynamic multiplicity* and refers to the fact that at the same operating conditions the hydrodynamic parameters can have multiple values. Therefore, hydrodynamic

parameters are a function not only of the operating conditions, but also of the preconditioning and flow history of the bed (Van der Merwe, 2008). The significance is that an array of hydrodynamic values can be achieved for a single velocity. To achieve the maximum and minimum values of the hydrodynamic parameters different pre-wetting procedures need to be followed (Loudon *et al*., 2006). The two main pre-wetting procedures used in laboratory studies are Levec and Kan. From previous studies it was found that the upper boundary for wetting and liquid-solid mass transfer is achieved in the Kan pre-wetting procedure and the lower boundary when the Levec pre-wetting method is applied (Van der Merwe, 2008). The procedures are as follows:

- *Levec mode*: The bed is flooded at low liquid velocities (u < 1 mm/s) under no gas flow. Once the bed has been flooded, it is drained and left for 30 min to drain completely. The liquid and gas are then reintroduced into the bed (Levec *et al*., 1988).
- *Kan mode*: The liquid velocity is increased until the pulsing regime is reached and the bed is then operated in the pulsing regime for 15–30 seconds. After this the liquid velocity is decreased to the operating velocities (Kan & Greenfield, 1983).

The difference in the hydrodynamics is caused by differences in the particle-scale liquid flow structures. For the trickle flow regime (LIR) the two dominant flow structures are film flow and filament/rivulet flow (Van Houwelingen, 2006). *Film flow* is where the liquid flows in a thin film over the particle and as the liquid flow rate is increased, this film expands to cover more of the particle. *Rivulet flow* is where the liquid flows over the particle in a stream of variable thickness and as the liquid velocity is increased, the rivulets only grow in thickness and do not necessarily increase the particle coverage.

For the Levec method the flow structure is dominantly rivulet flow, and as the liquid velocity is increased, the rivulets grow in thickness but no new rivulets are formed (Sederman & Gladden, 2001). This flow structure leads to a bed with pores that are filled completely with either liquid or gas, causing low liquid-gas interfacial area and poor liquid distribution in the bed.

For Kan pre-wetting the primary flow structure is film flow in the top of the bed, but rivulets are formed in the bottom of the bed (Van Houwelingen, 2006). This is characterised by higher wetting efficiency since a better spread of liquid over the particle is achieved.

2.3. *Required bed depth in trickle flow*

The first investigations done into the bed length variations of trickle flow were primarily on liquid distribution within the bed and the effect of particle shape and size. In these studies the liquid distribution in the bed was measured using an annulus collection method at the exit of the column. Herskowitz and Smith (1978) employed a point source to study the effect that the particle shape, particle size, column dimensions and liquid properties have on the liquid distribution within the bed. The first finding was that if the column diameter increased from 40.5 mm to 114 mm, the depth required for stabilisation of the liquid distribution increases. In order to compare different studies, the results needed to be compared on the basis of a dimensionless scale, the x/D ratio. Once this scaling had been done, both columns required the same x/D for stabilisations. The smaller column required a stabilisation depth of 6,5 and the larger column required a stabilisation depth of 6,1. Further investigation found that if the point source was replaced with a multi-point distributor, the depth required for stabilisation decreased to 4,3 for the large column and to 4,6 for the smaller column. Particle shape and size had no significant effect on the stabilisation depth with regard to the distributor; however, Herskowitz and Smith (1978) suggested that spherical particles aid the distribution within the bed. It should be noted that this study assumed that the external wetting had stabilised once the liquid distribution had stabilised, and also that the particles used were solid particles. Reis (1967) performed a similar study on structure packing in a column with a diameter of 400 mm and found that the liquid distribution had stabilised at an x/D value of 1,2. This was done with a multi-point distributor that had a drip point density of 4 222 drops/m^2, approximately ten times higher than that used by Herskowitz and Smith (1978).

In a review article by Gianetto *et al.*(1978) it was stated that the wetting in the bed can be improved if the distributor is properly designed. For further information on distributor design and types of distributor, refer to the review article by Maiti and

Nigam (2007). This article has a vast amount of information regarding the evolution of distributor design in trickle beds. It should be emphasised that if the aim is to study the effects of bed depth, all the external factors that can lead to maldistribution should be eliminated, such as a poorly designed distributor. The liquid distribution in a TBR does not depend only on the liquid distributor design, but also on the shape and size of the catalyst, the superficial velocities of the liquid and gas, and the physical properties of the liquid (Kundu *et al*., 2001). These properties affect the percentage of wall flow that takes place in the reactor.

Baussaron *et al.* (2007a, b & c)

These authors studied the effect of the liquid phase's affinity to the solids phase on the wetting efficiency, as well as how the wetting efficiency or liquid distribution varies as a function of the bed depth. For this study porous alumina particles were used and the particle diameter was varied between 3 mm and 6 mm. The length of the column was 0,35 m and it had a diameter of 0,057 m. This resulted in an L/D ratio of 7 and a D/d_p ratio of 16. (The D/d_p ratio is the ratio of the column diameter to the particle diameter). The study employed a multi-source distributor with an overall drip point density of 19 202 drips/m^2. Ethanol/water mixtures and pure heptane were used as the liquid phase and nitrogen as the gas phase. The wetting efficiency was measured by using a dye-adsorption technique.

For this technique dye is injected into the bed, after 5 minutes the injection of the dye is stopped and the bed is then operated for another 5 minutes to ensure that all unabsorbed dye is washed out. The bed is pushed up and out from the bottom, section by section, and at various depths photographs are taken and processed in order to calculate the wetting. This is a very tedious and destructive method of measuring the external wetting in a column.

The main finding of this study was that the wetting efficiency stabilised at a very shallow depth of an x/D of 1, for a pre-wetted bed. The pre-wetting method employed was the Kan mode. For the non-pre-wetted bed the wetting efficiency increased in the top section of the bed and then decreased with no sign of stabilisation, as seen in Figure 1.

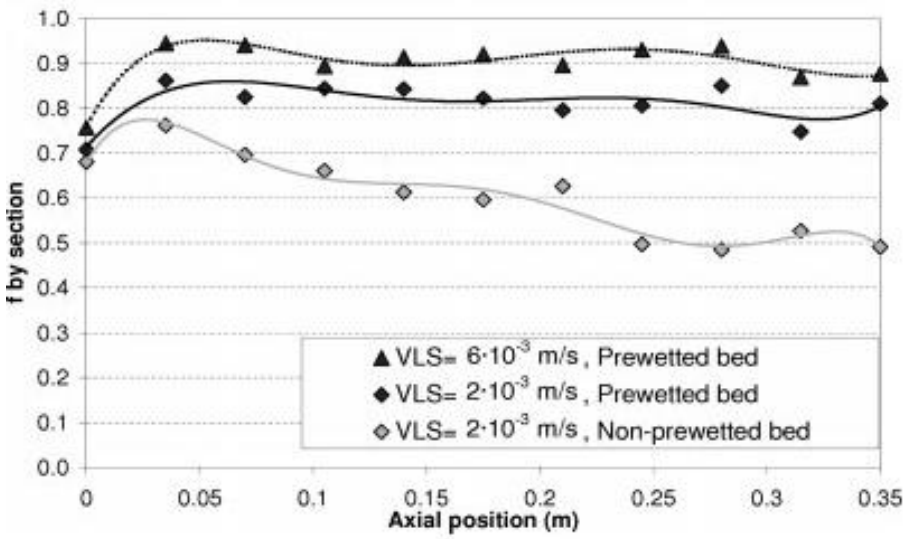

Figure 1: Axial variations in the wetting efficiency (Baussaron et al., 2007a, b & c)

Dang-Vu *et al.* (2006)

In this study the electrochemical method was employed to measure the liquid-solid mass transfer coefficient in a packed bed of Pall rings with an average diameter of 25,6 mm. The aim was to improve the correlation for the maldistribution factor in packed columns and to investigate the effect that liquid distribution has on hydrodynamic parameters such as liquid-solid mass transfer. The set-up used for this was a PVC tube with a diameter of 0,3 m and a bed depth of 2,1 m. This resulted in an L/D ratio of 7 and a D/d_p ratio of 12. This agrees reasonably well with the ratios used in the study by Baussaron *et al.* (2007a, b & c).

The main findings of this study were that as the distribution approaches uniformity, the depth required for stabilisation decreases. Three different types of distributor were employed: a single source, a cross-flow distributor and a ladder distributor. This resulted in a variation of the drip point density ranging from 1 to 466 drips/m^2. As the drip point density is increased, the depth required for the liquid-solid mass transfer to stabilise decreases from an x/D ratio of 5,5, for the point source to 4,9 for the ladder-type distributor. It should also be noted that although this column ratio is similar to that of Baussaron *et al.* (2007a, b & c), there is a massive difference in the drip point densities of the two columns, namely 19 202 versus 1 466.

Gostick *et al.* (2003)

This study employed the electrochemical method for measuring the mass transfer coefficient at various depths. The experimental set-up consisted of a PVC tube with an internal diameter of 0,3 m and a packed bed height of 1,65 m, which resulted in an overall x/D ratio of 5,5. This column was packed with 25,6 mm stainless steel Pall rings, some of which were coated in a polymer paint to ensure that the electrodes did not short-circuit in the bed. The pre-wetting mode used for this experiment was the Kan pre-wetting mode.

Gostick *et al.* (2003) found that a maximum point in the liquid-solid mass transfer coefficient was at an x/D value of 1,5, as seen in Figure 2. This corresponds to the minimum point found in the maldistribution study also done by Gostick *et al.* (2003). As can be seen from Figures 2 and 3, the liquid distribution within the bed is improved by the packing and a maximum liquid distribution is reached at an x/D ratio of 1,5. After the 1,5 maximum point, the liquid-solid mass transfer coefficient starts decreasing at a steady rate until an x/D of 4,5 is reached. After this value, the liquid-solid mass transfer is assumed to have stabilised. From an evaluation of Figure 2 it becomes clear that between 4,5 and 5,5 the rate of decrease has stopped, but the mass transfer has not stabilised although it was claimed that the liquid-solid mass transfer stabilised after 4,5. Gostick *et al.* (2003) proposed a hypothesis for this reduction in the liquid-solid mass transfer. As the radial spreading of the liquid progresses down the bed, the energy of the liquid is transferred into the radial direction and will result in lower linear velocities in the bed which decreases the mass transfer rate. Van Houwelingen (2006) suggested that the Kan mode tends to rivulet flow at the exit of the bed. Rivulet flow tends more to a Levec-type mass transfer coefficient, which is lower than the Kan mass transfer (Louden *et al.,* 2006). Figure 4 shows that the mass transfer in the outer zone of the bed is increasing, but this can be attributed to the fact that the liquid is spreading to the wall of the column.

For the point source work it was found that even after the liquid distribution had stabilised in the column, the liquid-solid mass transfer showed no signs of stabilisation. The multi-point distributor had a drip point density of 219,3 drips/m^2.

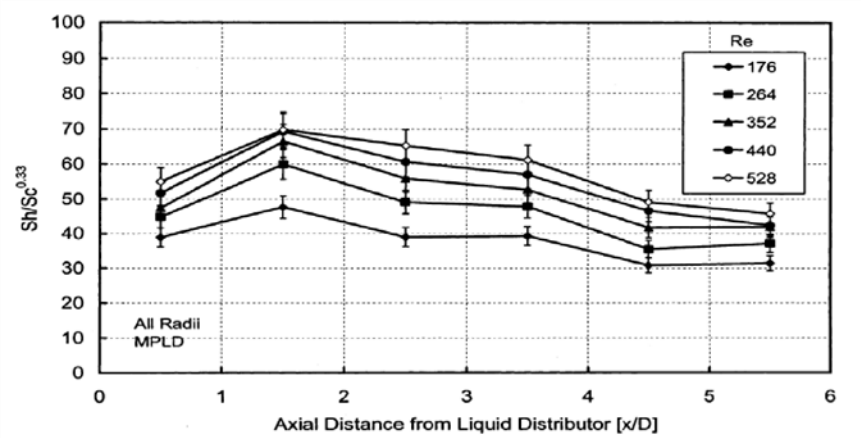

Figure 2: Axial variations in the liquid-solid mass transfer for a multi-point liquid distributor; 25,6 mm Pall rings were used (Gostick *et al.*, 2003)

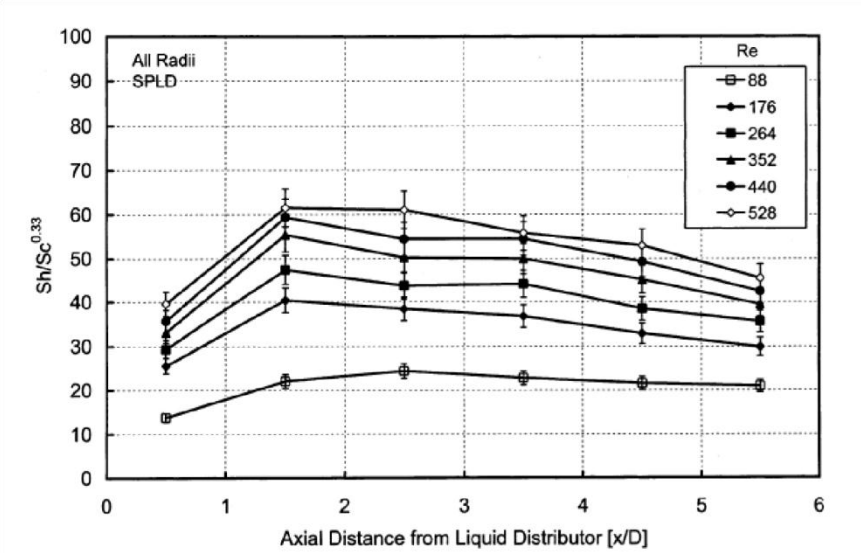

Figure 3: Axial variations in the liquid-solid mass transfer for a single-point liquid distributor (SPLD); 25,6 mm Pall rings were used in this study (Gostick *et al.*, 2003)

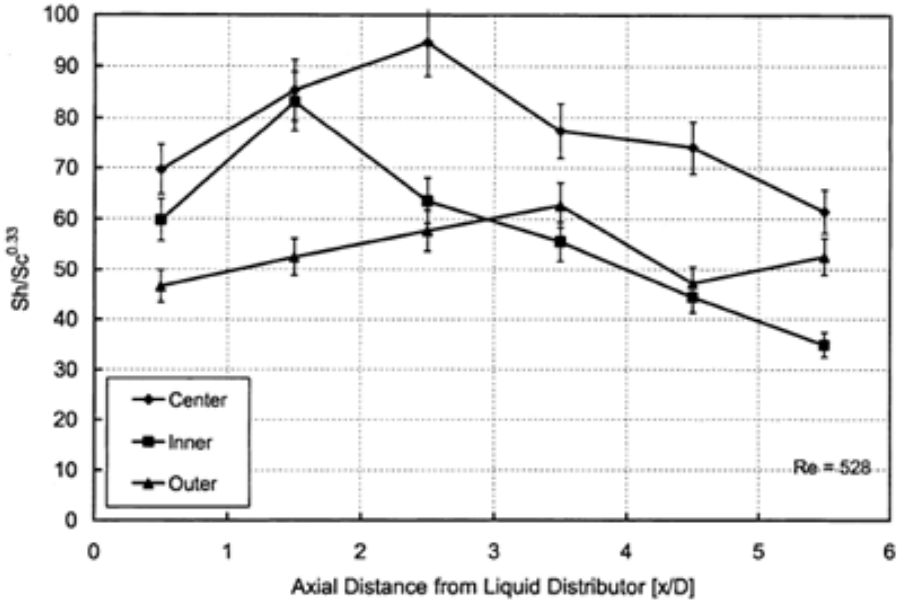

Figure 4: Variations in the liquid-solid mass transfer for a multi-point distributor at various depths and at various zones (Gostick *et al.*, 2003)

Schubert *et al.* (2008)

This study used high-definition gamma X-ray tomography to study the effect that particle porosity has on liquid saturation in the bed. The liquid distribution in the top of the bed was also varied to see what effect the initial distribution has on the liquid spreading in the bed. The experimental set-up consisted of an acrylic tube with an internal diameter of 90 mm and an overall length of 600 mm. This relates to an x/D ratio of 6,67 and a D/d_p ratio of 22,5. Glass packing and porous packing were used and for glass packing it was found that as the velocity of the liquid increased, the number of liquid channels increased. At low velocities the liquid channelling was primarily isolated to the wall region. For the porous particles it was found that the liquid distribution was more uniform and the amount of channelling was far less than with the non-porous glass particles. The more even spreading of the liquid channels over porous packing is the result of the internal wetting and capillary forces. Figure 5 shows the experimental results obtained by Schubert *et al.* (2008), from which it can be seen that for the porous particles at high and low liquid flow the stabilisation depth required was 50 mm (x/D of 0,5). However, for the glass particles it can only truly be said that the liquid saturation has stabilised at 150 mm (x/D = 1,6), although there

are still fluctuations in these measurements after a 150 mm depth for the high flow rate. At the low flow rate the glass particles did not stabilise completely.

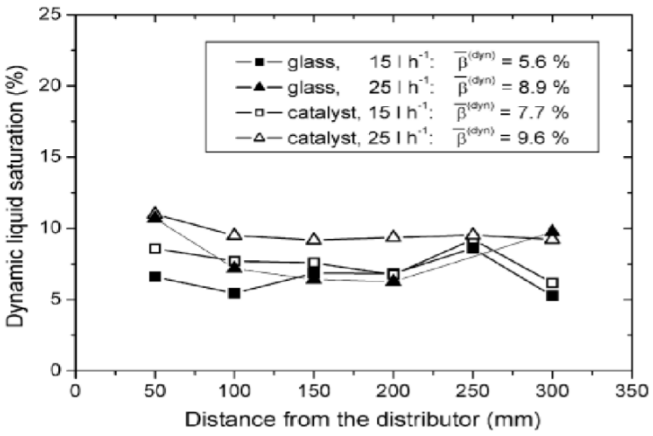

Figure 5: Axial profile of the liquid saturation of the bed (Schubert *et al.*, 2008)

Du Toit *et al.* (2014)[3]

Please note that when reference is made to this study, it is applicable only to the short column data, whereas the results of the current study are used for the long column. By employing the classic potassium ferrocyanide-ferricyanide electrochemical method Du Toit *et al.* (2014) measured the liquid-solid mass transfer and external wetting at various bed depths in order to investigate whether the hydrodynamics had stabilised. The column was a 2 m PVC tube with an internal diameter of 63 mm. This resulted in an x/D ratio of 31,75 which was deeper than that of any previous study. The packing material consisted of 4 mm solid glass beads, and 4,5 mm nickel-plated steel beads were used as the electrodes. This led to a D/d_p ratio of 21. The upper (Kan mode) and lower (Levec mode) hydrodynamic states were investigated.

The results of this study showed major deviations in the hydrodynamic parameters and both pre-wetting modes showed no signs of stabilisation. This result is in direct contrast with the results of Baussaron *et al.* (2007) and Schubert *et al.* (2008). If the two pre-wetting modes are compared, it is seen that the deviation in the external wetting efficiency of both modes is significant. For the mass transfer, however, this is

[3] Du Toit *et al.* (2014): This refers only to the data in the short column in the article, whereas the results of the current study were used for the longer column.

not the case in that the decrease for the Kan mode is insignificant. Figure 6 shows the experimental data of the study. From this we can see that the Kan mode is a function only of the external wetting efficiency, whereas for the Levec mode it is clear that the neither the mass transfer nor the external wetting stabilised.

If these data are compared with those of Dang-Vu *et al.* (2006) and Gostick *et al.* (2003), it can be seen that the plateau reached between x/D = 4,5 and 5,5 may merely be a shift in the particle-scale wetting. The reason for this assumption is that in Figure 6a there is a complete change in the slope of the data after a depth of 0,5 m (x/D = 7,91) since above the 0,5 m point the slope is very shallow and after the 0,5 m point the slope of the line becomes steeper. This is not close to the 5,5 and 4,9 reported by Gostick *et al.* (2003) and Dang-Vu *et al.* (2006); they used Pall rings which are designed to improve the spreading of the liquid. This can be seen when Figures 2 and 3 are compared with Figure 6a. Table 1 is a summary of the all the studies discussed.

Table 1: Summary of findings of previous studies

Study	L	D	d_p	ρ_L	Particle	Findings	Personal Comments on Paper
Baussaron *et al.* (2007)	0,35	0,05	3 – 6	700–1 000	Porous	The wetting stabilised at L/D < 1 for pre-wetted particles.	The total length of the column that was used in this study was only 350mm. This allowed for an L/D ratio of 7 to be investigated. Also the method used was an invasive and destructive one that prevents repeatability to be studied.
Dang-Vu *et al.* (2006)	2,1	0,3	25,6	1 200	Pall ring	When the drip point density was increased from 1 to 466, the x/D for stabilisation decreased from 5,5 to 4,9.	This study used large Pall rings to investigate liquid solid mass transfer. The drip point density was also much lower than that of Baussaron *et al.* (2007)
Gostick *et al.* (2003)	1,65	0,3	25,6	1 200	Pall ring	Liquid distribution was found to have stabilised after an L/D of 1,5. The LSMT showed signs of stabilising after an x/D of 4,5.	Similar study than that of Dang-Vu *et al.* (2006). The findings were also similar. The authors only measured up to an x/D = 4,5, and then inferred liquid-solid mass transfer stabilised.
Schubert *et al.* (2008)	0,6	0,09	4	1 000	Porous Solid	The depth required for solid particles (x/D = 1,6) to stabilise is deeper than for porous particles (x/D = 0,5).	Investigated both porous and non-porous particles and found that porous particles will stabilise hydrodynamic parameters at lower x/D values than non-porous particles.
Du Toit *et al.* (2014)*	2	0,63	3	1 200	Solid glass	After a deep bed study, no stabilisation was found.	Found that the rate of decrease in LSMT and wetting changes after the x/D = 4,5. No stabilisation after the x/D = 17.

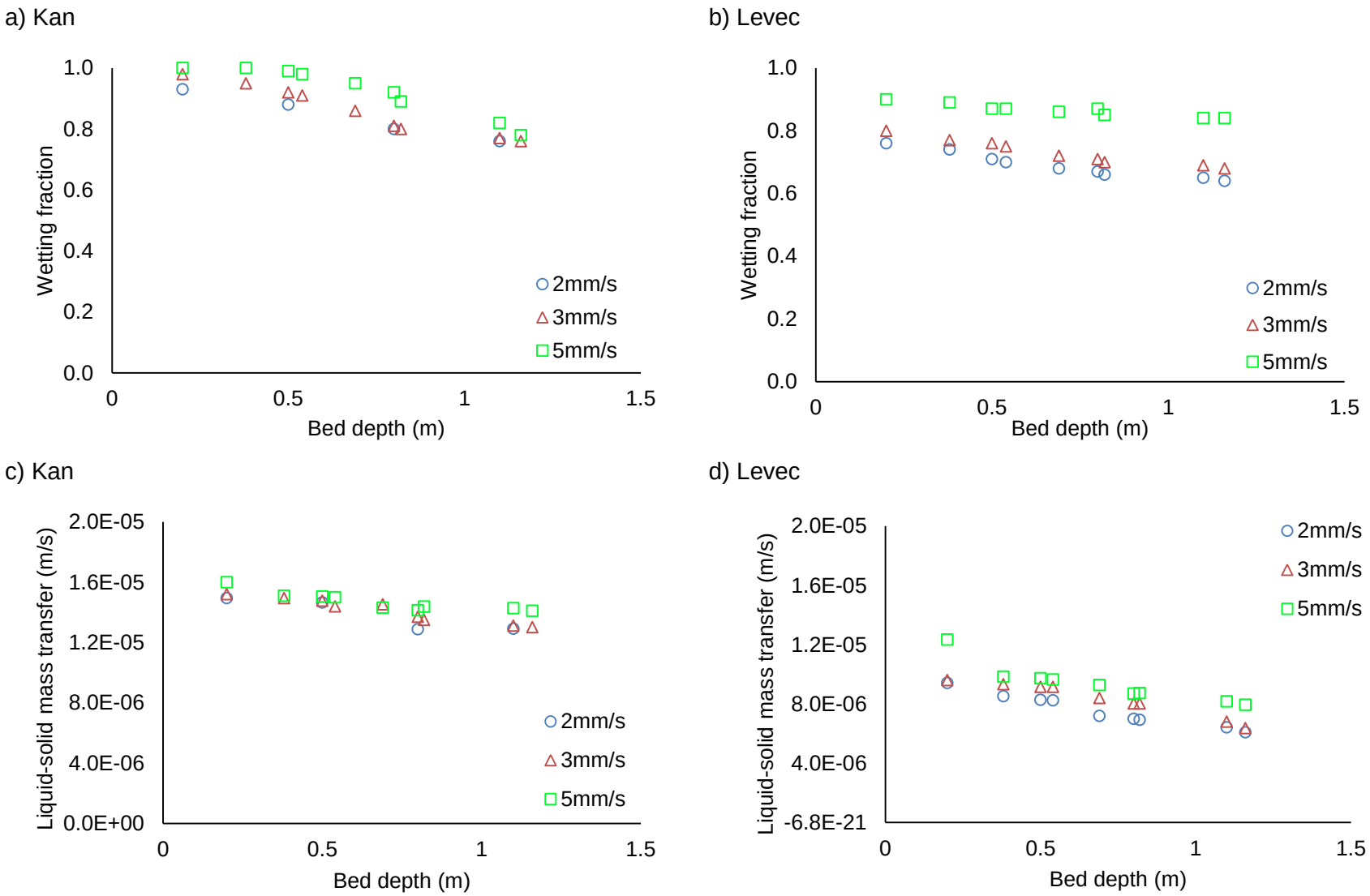

Figure 6: Experimental data for the study done by Du Toit *et al.* (2014). The figures on the left-hand side represent the Kan mode (a & c) and the figures on the right-hand side represent the data for the Levec mode (b & d)

2.4. *Method for simultaneous quantification of mass transfer and external wetting*

There are numerous methods for measuring the liquid-solid mass transfer and the wetting efficiencies (Baussaron *et al.,* 2007; Joubert & Nicol, 2009; Van Houwelingen *et al*., 2006). Until recently no method was able to measure both of these hydrodynamic parameters simultaneously since the liquid-solid transfer rate is directly affected by the wetted area. However, Joubert and Nicol (2013) employed the well-known electrochemical method and found that by adjusting the applied voltage, the liquid-solid mass transfer and the wetting could be measured simultaneously. The electrochemical method can measure both the wetting and the liquid-solid mass transfer under same flow conditions and with the same liquid properties.

Vogtländer & Bakker (1963) employed the redox reaction of potassium ferricyanide-ferrocyanide to measure mass transfer fluctuations at the wall of a pipe for turbulent flow; sodium hydroxide was used as a supporting electrolyte. The reason for selecting the ferricyanide-ferrocyanide redox couple is that it has the highest reaction rate constant (Eisenburg *et al.*, 1955). The best electrodes to use are either nickel or platinum (Vogtländer & Bakker, 1963). It is also recommended that the electrolyte be kept under a nitrogen atmosphere to avoid the oxidation of the ferrocyanide and to strip dissolved oxygen from the solution to ensure that no side-reactions can take place on the electrode (Reiss & Hanratty, 1962; Vogtländer & Bakker, 1963). Preliminary tests showed that commercial-grade ferricyanide and ferrocyanide have an active life time of about one week. However, it is best not to use a batch for more than four days (Rao & Drinkenburg, 1985). The two reactions taking place in the system are:

$$\text{Cathode (test electrode): } Fe(CN)_6^{3-} + e^- \rightarrow Fe(CN)_6^{4-}$$

$$\text{Anode (reference electrode): } Fe(CN)_6^{4-} \rightarrow Fe(CN)_6^{3-} + e^-$$

To ensure that the test electrode is the limiting electrode, the anode area has to be larger than the cathode area. This is achieved by either doubling the area of the anode (Vogtländer & Bakker, 1963) or quadrupling the area (Joubert & Nicol, 2009, 2013). Nicol and Joubert (2013) found that at low voltages all the velocity lines

merge, below 50 mV. The reason for this merge is that the electrochemical reaction shifts from being a mass transfer-limited rate to a kinetics-limited rate. The kinetics-limited rate is a function of the area. Table 2 is a summary of previous studies that employed the electrochemical method and the concentrations used.

Table 2: Summary of previous studies that employed the electrochemical method with the electrolyte composition

Study	$K_3Fe(CN)_6$ [M]	$K_4Fe(CN)_6$ [M]	NaOH [M]
Reiss & Hanratty (1962)	0,1–0,01	0,1–0,01	2
Vogtländer & Bakker (1963)	0,025	0,025	0,5
Mitchell & Hanratty (1966)	0,01	0,1	2
Jolls & Hanratty (1969)	0,01	0,01	1
Rao & Drinkenburg (1985)	0,006	0,05	1
Bartelmus (1989)	0,01	0,05	0,5
Sims, Schulz & Luss (1993)	0,01	0,0125	1
Gostick *et al.* (2003)	0,0038	0,004	0,5
Dang-Vu *et al.* (2006)	0,0036	0,004	0,5
Joubert & Nicol (2009)	0,003	0,02	1

$$N = \left(\frac{I_{lim}}{AF}\right)(1 - T) \quad (1)$$

$$K_{ls} = N/(C_B - C_W) \quad (2)$$

$$I_{lim} = K_{ls} C_B A F \quad (3)$$

$$A = f A_t \quad (4)$$

Equation 1 is used to relate the current (I) to the rate of reaction per unit area (N) and T is the transfer number. At low ferricyanide concentrations T = 0.001. Equation 2 defines the mass transfer coefficient as a function of the bulk concentration (C_b) and the surface concentrations (C_w). At higher voltages (700–1 000 mV) $C_w \approx 0$. By combining equations 1 and 2, equation 3 is derived. This equation is used to relate the current to the mass transfer coefficient, where F is the Faraday constant and A is the wetted area of the electrode, which is calculated using equation 4 (Mitchell & Hanratty, 1966).

2.5. *Objective of Study*

Table 1 is a summary of the most recent studies done on the effect of bed length on external wetting and liquid-solid mass transfer. From Table 1 it is seen that there is still no single finding on whether the liquid-solid mass transfer or wetting efficiency has stabilized after a certain bed depth. Du Toit *et al*. (2014)* showed that even a deep bed study (x/D = 17) the hydrodynamic parameters has not stabilised.

This study presents the longest column ever employed for a hydrodynamic study. The column was 5 m long. Due to space constraints a 5m column was employed.

3. Experimental

3.1. Experimental set-up

Figure 7 is a schematic drawing of the experimental set-up that was designed to measure the liquid-solid mass transfer coefficient and external wetting efficiency at various bed depths. All experiments were carried out at atmospheric temperatures and pressures. The column was a 5 m clear PVC tube with an internal diameter of 105,3 mm; 4 mm glass beads were used as packing material. The D/dp ratio of the column was 26,3 which is above the minimum suggested value of 25 (Al-Dahhan *et al.*, 1995). Wall flow for this column was assumed to be negligible. The LSMT and wetting can be measured to a bed depth of 3,5 m (see Figure 10).

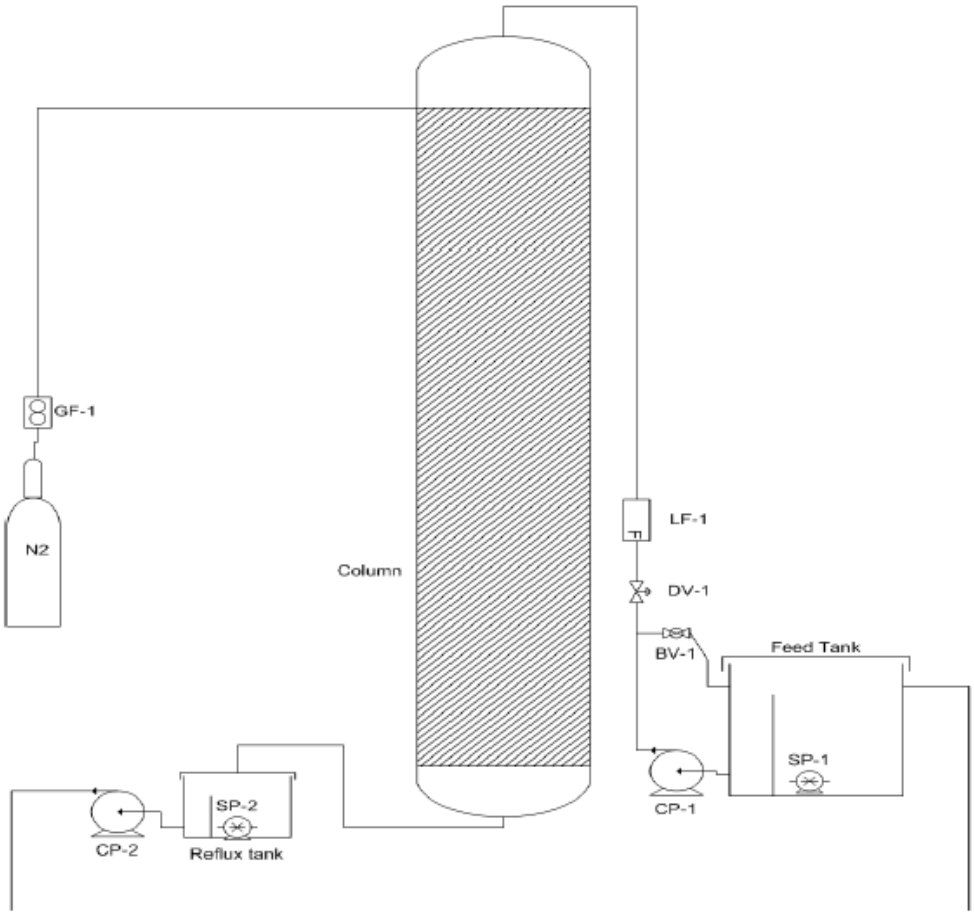

Figure 7: Experimental set-up

The feed tank and reflux tank were designed with submersible pumps (SP-1 and SP-2) and weirs. This allows the centrifugal pumps (CP-1 and CP-2) to operate at a

constant head. The valve BV-1 is a kickback valve to ensure that a minimum flow of CP-1 is achieved and the flow is controlled by DV-1. The liquid flow rate was measured using an electromagnetic flow-measuring system, the PROline promag 10H from Endress and Hauser. The gas feed was controlled with a Brooks Smart Mass Flow Controller 5851S. The range for the gas controller was 0–100 ℓ/min and the controller was calibrated for nitrogen. For this experiment the gas flow rate was fixed at 20 mm/s.

The liquid was fed to the column through a needle distributor. Figure 8 is a schematic drawing of the distributor. The needles were made from 3 cm pieces of ¼" stainless steel tubes. They were placed in a square pitch with ½" spacing between the centre of each hole, giving a drip point density of 10 280 drips/m^2. Liquid distribution has a significant effect on the overall liquid-solid mass transfer value since it directly affects the wetting efficiency of the bed (Dang-Vu *et al*, 2006). A key design parameter for a liquid distributor is that the drip point density should be more than 5 000 drips/m^2 as suggested by Burghardt *et al.* (1995). Bonilla (1993) suggested a general rule for a well-designed distributor: the outer 10% near the wall of the column should receive 10% of the feed. The greyed area in Figure 8 represents the outer 10% of the column area, and it can be seen that 10% of the flow is sent to the wall of the column.

The gas enters the column below the distributor, and is fed through three ¼" inch stainless steel tubes spaced at 120° angles from each other around the column. The column was pre-wetted by either the Levec or the Kan pre-wetting modes. The liquid velocities investigated were 2, 3 and 5 mm/s to be comparable with the results of Du Toit *et al.* (2014).

In the Levec pre-wetting mode the liquid flow is set to a low velocity (± 1 mm/s) and the exit of the column is closed. The column is then flooded, with the low liquid velocity ensuring that no bubbles are trapped inside the bed. Once the bed is completely flooded, the liquid feed is switched off and the exit re-opened. The bed is then drained for 30–35 minutes before liquid is reintroduced. The flow rates in the column were allowed to stabilise for 5 minutes before the LSMT and wetting were measured.

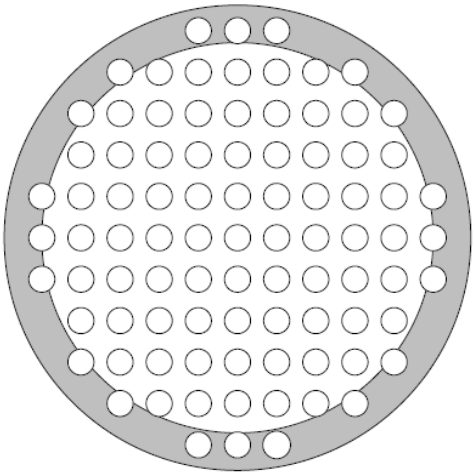

Figure 8: Distributor design for this experiment

In the Kan pre-wetting mode the liquid and gas velocity are increased until the pulsing regime is reached. The column is operated in the pulsing regime for 30 seconds, after which the liquid and gas velocities are decreased to the desired values. Once the flow has stabilised, measurements are taken.

3.2. The electrochemical method of measuring both LSMT and wetting

Distilled water was used as a solvent with a mixture of potassium ferricyanide and potassium ferrocyanide as the electrolyte, and sodium hydroxide as the supporting electrolyte. The reduction of ferricyanide occurs at the cathode (reaction I) and the reverse reaction occurs at the anode when a voltage is applied over the electrodes.

$$Fe(CN)_6^{3-} + e^- \rightarrow Fe(CN)_6^{4-} \qquad \text{I}$$

The cathodes were placed inside the bed and consisted out of 4 500 nickel-plated steel beads with a diameter of 4.5 mm. The axial distances between two cathodes were 0.5 m, and 4 mm glass beads acted as isolation in between the cathodes (see Figure 10). To avoid interference from the anode at the bottom of the column, the distance between the last cathode and the anode was increased to 1,5 m. This was done because a residual charge can build up on the anode. The distance between the top of the bed and the first cathode was 300 mm, thus 500 mm below the distributor. In Figure 10 the line at the top of the column represents the distributor. The anode is located at the exit of the column and consisted of 13 500 nickel-plated steel beads. This amount ensures that the limiting area is the cathode and not the

anode. The composition and physical properties of the electrolyte are given in Tables 3 and 4 respectively.

Table 3: Composition of the electrolyte

Species	Concentration
$K_4Fe(CN)_6$	0,003 M
$K_3Fe(CN)_6$	0,02 M
NaOH	1 M

Table 4: Physical properties of the electrolyte

Property	Value	Units
Density	1 020	kg/m^3
Viscosity	0,0019	Poise
Surface tension	25,5	Dynes/cm
Diffusion coefficient	$6,49 \times 10^{-9}$	m^2/s

Figure 11 shows that the current reaches a plateau in the voltage range of 2.5–3 V. This is where the reaction is mass transfer limited. All LSMT measurements were taken at 2.9 V. Equation 4 is used to relate the measured current to the liquid-solid mass transfer.

$$I_{\lim} = nK_{ls}fAFC \quad (5)$$

$$f = \frac{I_{lim}}{I_{4500}} \quad (6)$$

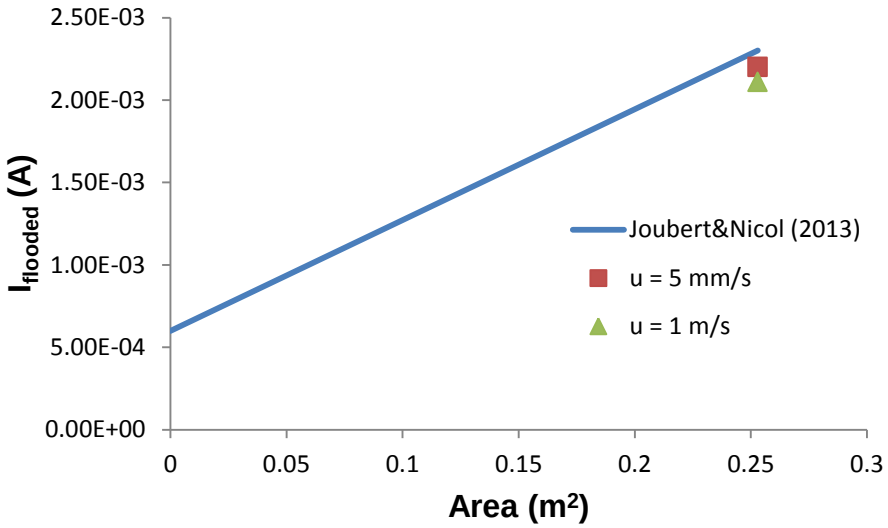

Figure 9: Calibration run for the wetting measurements

As mentioned before, Joubert and Nicol (2013) found that the liquid velocity has no effect on the current at low voltages. If the applied voltage is below 50 mV, the current depends on the wetted area. When the bed is operating at 20 mV, the wetting can be calculated using equation 5, where I_{4500} is the measured current for a bed that is operated in a flooded mode, with 100% wetting efficiency.

The study by Joubert and Nicol (2013) used different electrode areas to calibrate the current as a function of the total electrode area. It was found that the current was a linear function with area. Since the study by Joubert and Nicol (2013) stopped at an area of 0.225 m^2 (4 000 beads), the data had to be extrapolated to an area of 0.253 m^2 (4 500 beads), as seen in Figure 9. Two test runs at 1 mm/s and 5 mm/s were done with 4 500 beads to verify the extrapolation. From the extrapolated data it was found that I_{4500} should be 2,32 mA. However, for the test runs the current values were 2,11 mA and 2,2 mA at 1 mm/s and 5 mm/s respectively. The deviation between the measurements of the two runs was 4%.The deviation between these two runs and the extrapolated data from Joubert and Nicol (2013) was 5% at 5 mm/s and 9% at 1 mm/s. The average current between the 1 mm/s and 5 mm/s is taken as the I_{4500} current.

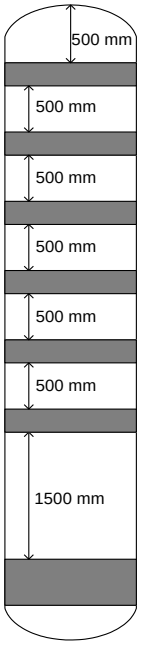

Figure 10: Electrode placement within the bed

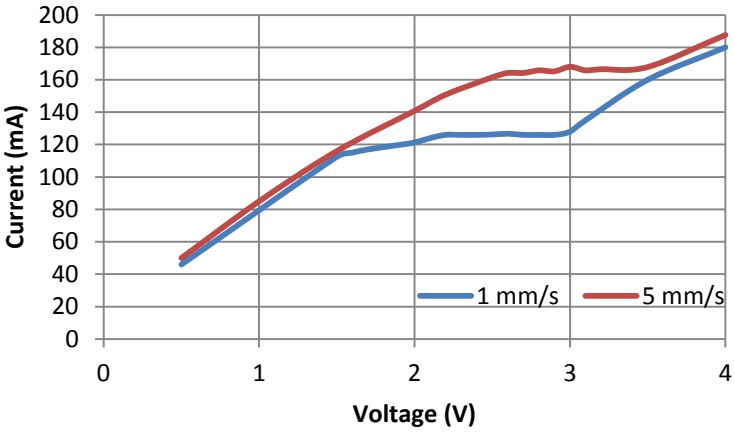

Figure 11: Current response of the electrochemical reaction

4. Results and Discussion

4.1. Repeatability

Al-Dahhan *et al.* (1995) reported that the repeatability between two randomly packed beds can vary between 10 and 20%. For this reason the decision was made not to repack between runs. The bed would only be drained and dried after each run. The results of the two runs are given in Figures 12 to 15. It can be seen that the runs show good repeatability. The variation in the measurements of the Levec mode is less than those of the Kan mode. Table 5 shows the deviation for both liquid-solid mass transfer (LSMT) and external wetting efficiency for both the Levec and Kan modes.

Table 5: Average deviation between the first and second runs

Velocity	Kan mode		Levec mode	
	Wetting	LSMT	Wetting	LSMT
2 mm/s	10,1%	8,5%	3,9%	9%
3 mm/s	3,4%	4,9%	4,4%	7,6%
5 mm/s	2%	7,4%	3,8%	5,2%

4.2. Comparison between the Kan and the Levec pre-wetting modes

In liquid-solid mass transfer and external wetting studies, the upper hysteresis branch is achieved using the Kan pre-wetting mode, while the lower hysteresis branch is achieved using the Levec pre-wetting mode. Figures 16a and 16 b show the external wetting efficiencies found for both the Kan and Levec modes. For the Levec mode the wetting efficiency decreased monotonically with bed depth. Although the Kan mode showed initial signs of stabilisation, after 3 m the wetting efficiency started to decrease with increasing bed depth. Baussaron *et al.* (2007a, b & c) investigated the axial variation of wetting efficiency and found that if the bed is properly wetted, the external wetting efficiency stabilises; however, this was for porous catalyst particles and an aspect ratio (x/D) of 6,14. This ratio is in the region that showed stabilisation in this investigation, but porous catalyst additionally influences the wetting behaviour, potentially creating an offset at the point where the

wetting efficiency starts to decrease. From a previous study (Ravindra *et al.*, 1997) it is known that the Levec mode consists predominantly of rivulet flow and the Kan mode is a mixture of film flow and rivulet flow. Van Houwelingen (2006) discovered that at the exit of the column the Kan mode shifts to predominantly rivulet flow, while the upper section of the bed is predominantly film flow. This shift was also visually verified during the Kan runs of this study and could explain the decrease wetting efficiency beyond a certain bed depth.

LSMT coefficients are calculated using the measured wetting values and equation 5. In Figures 16c and 16 d the calculated LSMT values are shown and from Figure 16d it be seen that the liquid-solid mass transfer (LSMT) coefficient for the Levec pre-wetting mode decreased with axial distance from the distributor, whereas it increased with increasing superficial velocity. The Kan mode's liquid-solid mass transfer did not vary significantly with bed depth and also increased with increasing superficial velocity. The LSMT values of the Kan mode are generally also higher than those of the Levec mode. Based on the correlation of Duduković *et al.* (2002) it was expected that the increase in the LSMT with superficial velocity would be in the range of 2,2–2,5 times when going from 2 mm/s to 5 mm/s, whereas the actual increase between 2 mm/s and 5 mm/s was 1,6 for the Kan mode and 1,08 for the Levec mode. Trivizadakis and Karabelas (2006) suggested that an increase in the mass transfer is a function of increased interstitial velocity. The interstitial velocity can be calculated by dividing the superficial velocity by the liquid hold-up. Loudon *et al.* (2006) showed that the Kan mode had higher liquid hold-up than the Levec mode which will result in a lower interstitial velocity and mass transfer. However, these results and those of other previous studies (Du Toit *et al.,* 2014; Joubert & Nicol, 2013) showed the opposite trend in mass transfer. Therefore the suggested theory of Trivizadakis and Karabelas (2006) does not seem applicable to explain the deviations in mass transfer between the two pre-wetting modes.

In order to explain the variation between the two pre-wetting modes the surface renewal rate process is considered. Moccairo *et al.* (2013) suggested that three zones exist in a trickle bed: either completely dry, statically wetted or dynamically wetted. Nicol and Joubert (2013) proved this hypothesis to be true by using microelectrodes and the electrochemical method used in this investigation. These researchers also discovered that if a zone in the bed is static, it never becomes

dynamic and only grows in size with increased superficial velocity. Lastly, they observed that the static zones are more dependent on the liquid superficial velocity than the dynamic zones. When their observations are taken into consideration it can be seen in Figures 16c and 16d that the wetting is more dynamic for the Kan mode and more static for the Levec mode, since wetting is more dependent on the liquid superficial velocity for the Levec mode. Nicol and Joubert (2013) also observed that wetting efficiency for the Levec mode had a much higher percentage of static liquid on an area basis. For the Levec mode the decline in both the wetting and LSMT coefficient with bed depth indicates that the “quality” of the liquid flow in the bed has changed. It appears that more static liquid zones form and these results in a much lower surface renewal rate of the reacting anion. For the Kan mode the “quality” of the flow remains constant with bed depth and the dynamic liquid zones are replenished with reagents (the anions) at a faster rate. When we now consider the case of 2 mm/s in the Kan mode it can be concluded that the low LSMT values are due to a low interstitial velocity.

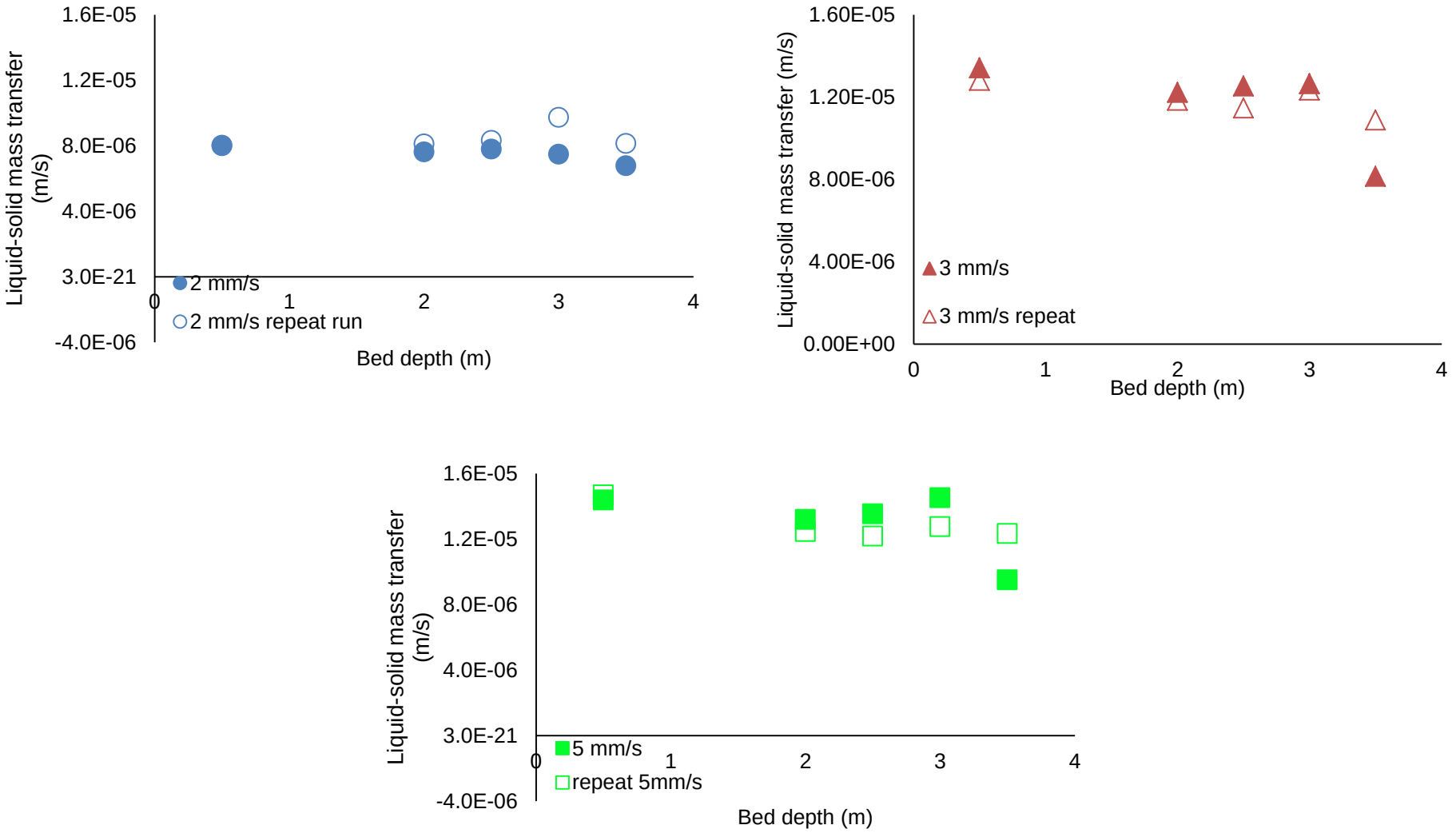

Figure 12: Liquid-solid mass transfer repeat runs for the Kan mode

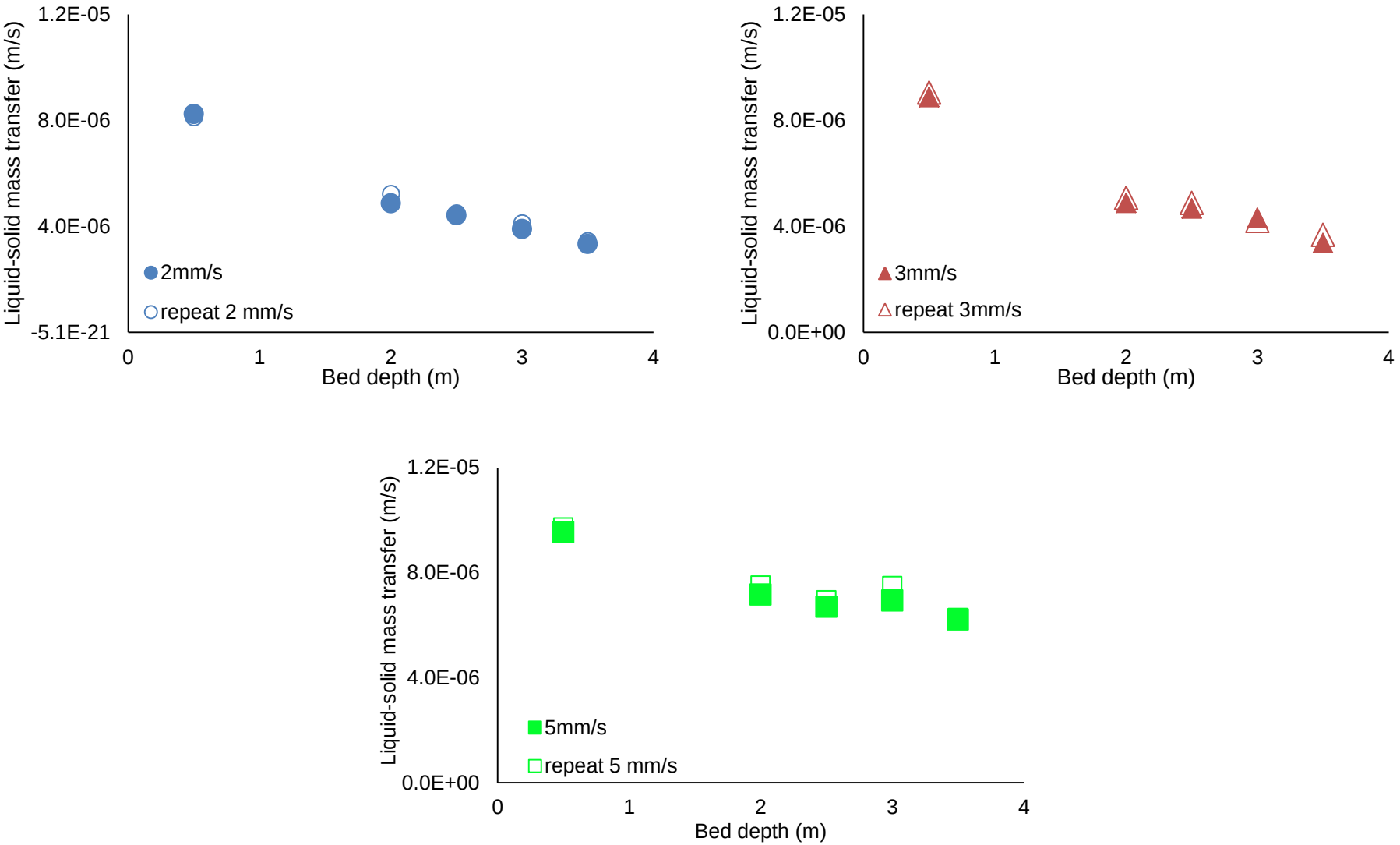

Figure 13: Liquid-solid mass transfer repeat runs for the Levec mode

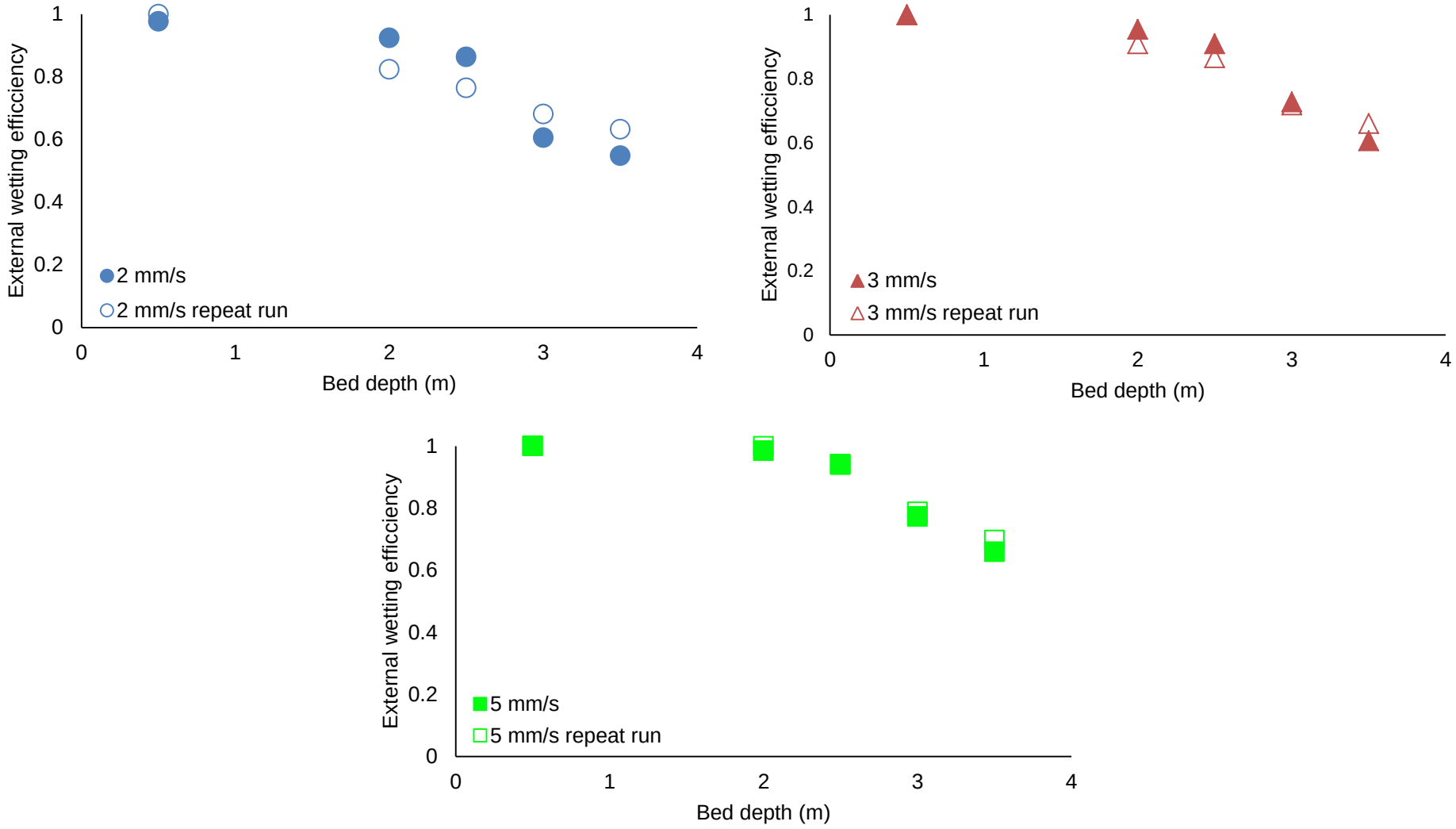

Figure 14: External wetting efficiency for the Kan mode

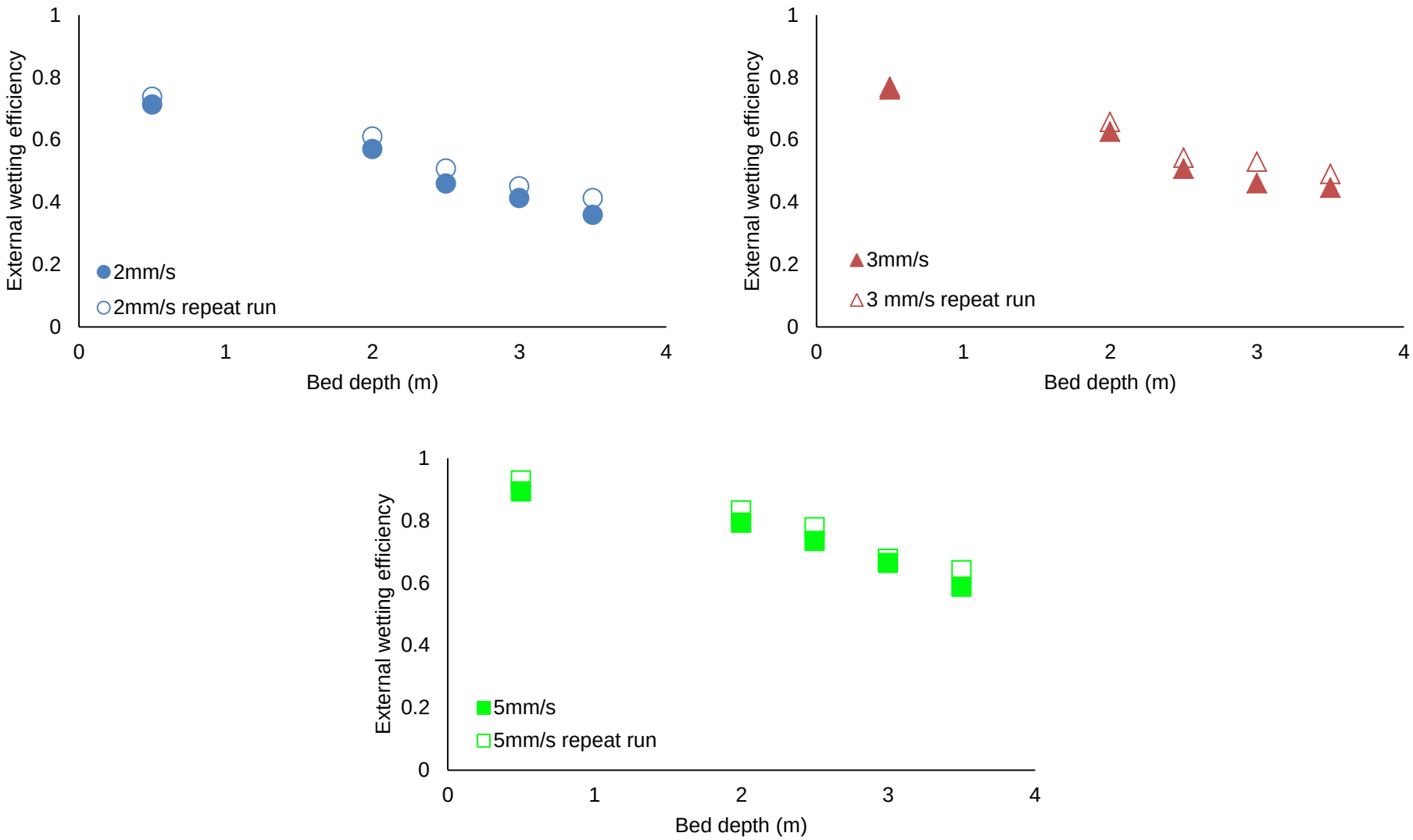

Figure 15: External wetting efficiency for the Levec mode

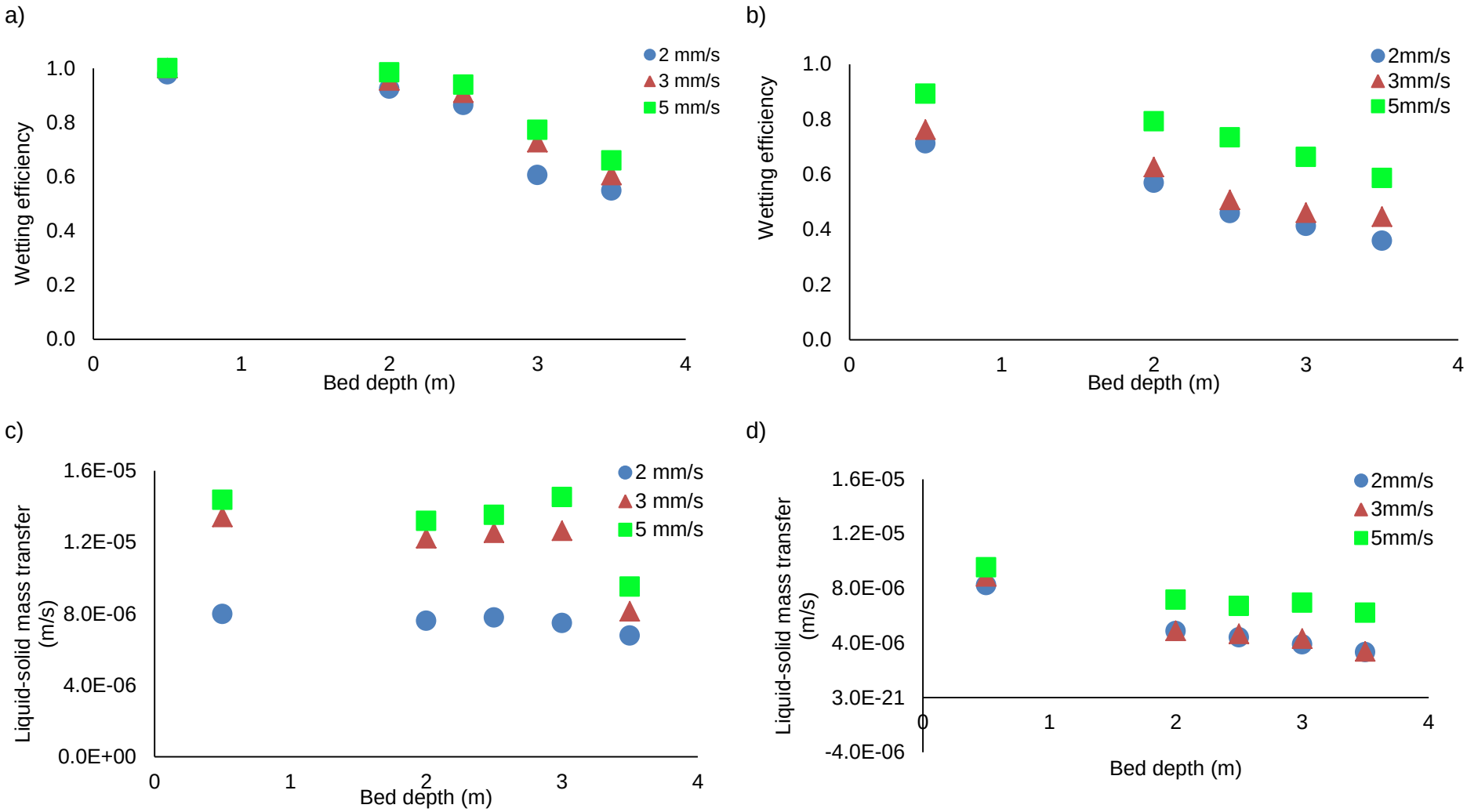

Figure 16: Experimental results. Kan mode results are on the left-hand side (a & c); Levec mode results are on the right-hand side (b & d)

4.3. Comparison of this study with that of Du Toit et al. (2014)[4]

When compared with the study by Du Toit *et al.* (2014)[4], it is seen in Figure 17 that the wetting efficiency for the Kan mode is a function of the length of the reactor. The wetting efficiency of both columns follows the same trend, i.e. it decreases rapidly near the exit of the column. In the results obtained by Du Toit *et al.* (2014)[4] there is a pinch point near the exit of the column and a similar result is seen in the data of this study. Figures 17b and 17d display a comparison for the Levec pre-wetting mode for this study and the study of Du Toit *et al.* (2014)[4]. From the trend it is seen that, unlike with the Kan mode, the wetting efficiency decreases linearly down the bed.

When looking at the average decrease for the Kan mode liquid-solid mass transfer, the decrease is 14%, similar to the findings of Du Toit *et al.* (2014)[4] where the decrease was 11%. This also confirms the finding that the Kan mode is affected by the length of the column. The decrease for the Levec mode liquid-solid mass transfer was 52%, which shows that for this mode the specific LSMT decreases as the bed length increases. Du Toit *et al.* (2014)[4] found the decrease to be 30% at a length of 1,6 m.

Du Toit *et al.* (2014)[4] state that these results only give insight into the hydrodynamics on a particle scale and are not an accurate representation of the particle wetting of an organic liquid on a porous catalyst, and the author concurs with this statement. Even though this study confirms the results of Du Toit *et al.* (2014)[4], it cannot clearly disprove the findings of Baussaron *et al.* (2007a, b & c) and Schubert *et al.* (2009) since both of these studies used porous packing material which affected the wetting behaviour. Further study is needed into the effect that the porosity of a particle has on the wetting efficiency with respect to bed length.

[4] Du Toit *et al.* (2014): This refers only to the data in the short column in the article, whereas the results of the current study were used for the longer column.

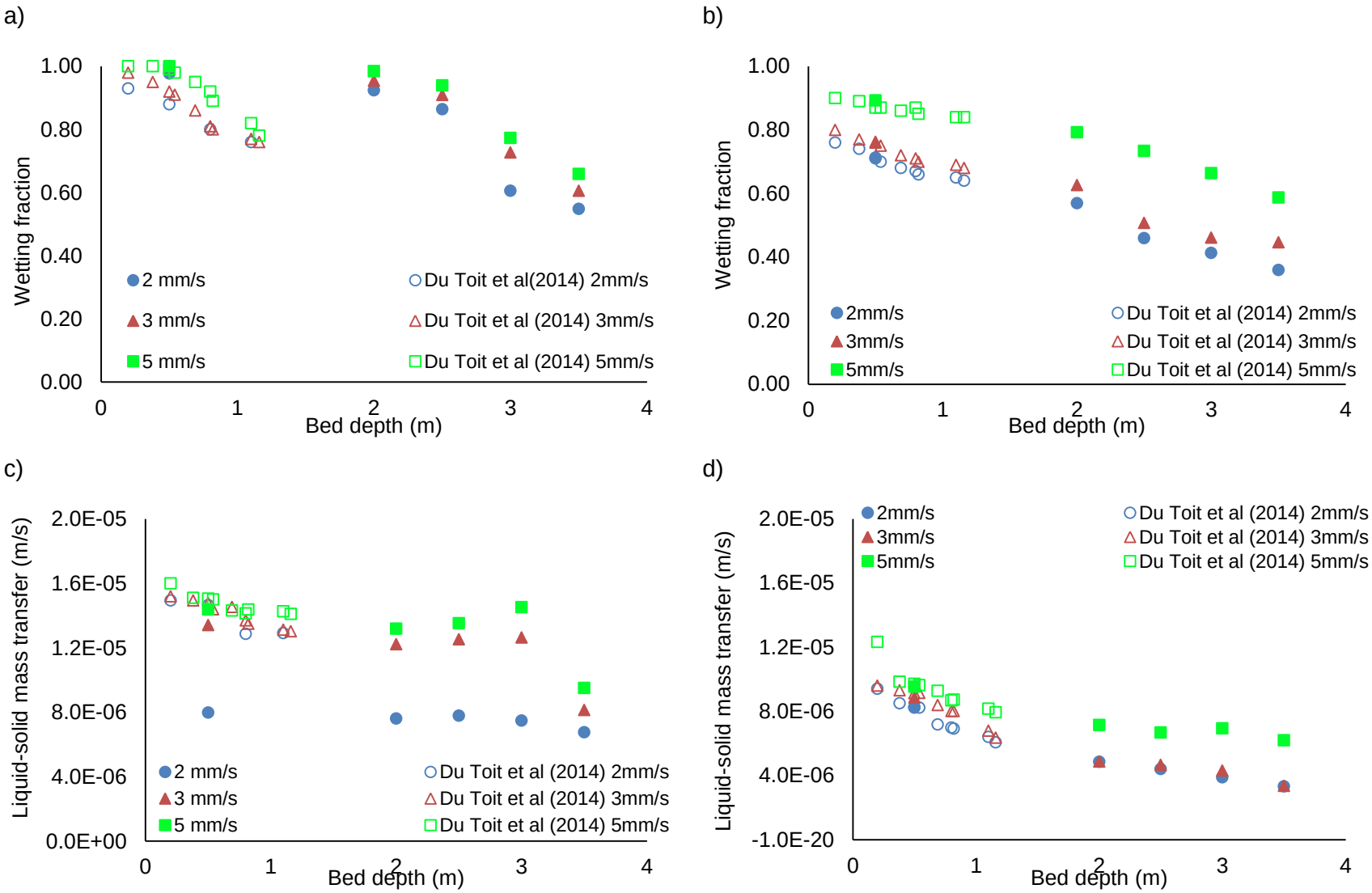

Figure 17: Comparison between this study and the study of Du Toit *et al.* (2014). Kan mode results are on the left-hand side (a & c); Levec mode results are on the right-hand side (b & d)

5. Conclusions

By using the new electrochemical technique developed by Joubert and Nicol (2013) the liquid-solid mass transfer and wetting efficiency could be measured simultaneously and separately under the same run conditions. This gave good insight into the axial variation of these two hydrodynamic parameters. Two different pre-wetting modes (Kan and Levec) were also employed to vary the hydrodynamic state of the bed.

Liquid-solid mass transfer and wetting efficiency were studied at both the upper branch and lower branch of the hydrodynamic envelope. For the upper branch of the envelope the wetting efficiency and liquid-solid mass transfer remained constant initially, but after 3 m the wetting efficiency decreased continually. The mass transfer decreased slightly by 14%, while the wetting efficiency decreased by 45%. For the lower branch of the hydrodynamic envelope the wetting efficiency and liquid-solid mass transfer decreased linearly to the column exit. The wetting efficiency decreased by 52% and the liquid-solid mass transfer decreased by 50%.

These results show the same trends as found by Du Toit *et al.* (2014)[5] and stand in direct contrast with the results of Baussaron *et al.* (2007a, b & c), Schubert *et al.* (2008) and Dang-Vu *et al.* (2006). Nevertheless, it should be noted that this study employed an inorganic liquid on non-porous particles, while the other studies used an organic liquid on porous particles.

[5] Du Toit *et al.* (2014): This refers only to the data in the short column in the article, whereas the results of the current study were used for the longer column.

6. References

Al-Dahhan, M. H., Duduković, M.P. (1995) “Catalyst wetting efficiency in trickle bed reactors at high pressure”. *Chemical Engineering Science,* 50(15), 2377–2389

Al-Dahhan M.H., Wu, Y., Duduković, M.P. (1995) “Reproducible technique for packing laboratory-scale trickle-bed reactors with a mixture of catalyst and fines”. *Industrial and Engineering Chemical Research*, 34, 741–747

Bartelmus, G., (1989) “Local solid-liquid mass transfer coefficient in a three phase reactor”. *Chemical Engineering Progression,* 26, 111-120

Baussaron, L., Julcour-Libigue, C., Wilhelm, A., Delmas, H. (2007a) “Wetting Topology in trickle bed reactors”. *American Institute of Chemical Engineers Journal*, 53, 1850–1860.

Baussaron, L., Julcour-Libigue, C., Boyer, C., Wilhelm, A., Delmas, H. (2007b) “Effect of particle wetting on liquid-solid mass transfer in trickle bed reactors” *Chemical Engineering Science*, 62, 7020–7025.

Baussaron, L., Julcour-Libigue, C., Boyer, C., Wilhelm, A., Delmas, H. (2007c) “Particle wetting in trickle bed reactors: Measurement techniques and global wetting efficiency”. *Industrial and Engineering Chemical Research*, 46, 8397–8405.

Bonilla, J.A. (1993) "Don't neglect liquid distributors". *Chemical Engineering Progression,* 89(3), 47–61.

Burghardt, A., Bartelmus, G., Jaroszynski, M., Kolodziej, A. (1995) “Hydrodynamics and mass transfer in a three-phase fixed-bed reactor with concurrent gas-liquid down flow”. *Chemical Engineering Journal*, 58, 83–99

Dang-Vu, T., Doan, H.T., Lohi, A., Zhu, Y. (2006) "A new liquid distribution factor and local mass transfer coefficient in a random packed bed". *Chemical Engineering Journal,* 123, 81–91.

Duduković, M.P., Larachi, F., Mills, P.L. (2002) “Multiphase catalyst reactors: A perspective on current knowledge and future trends”. *Catalysis Review*, 44, 123–246.

Dutkai, E. and Ruckenstein, E., (1968), “Liquid Distribution in Packed Column”. *Chemical Engineering Science*, 23, 1365-1373

Du Toit, E.L., Joubert, R., Saayman, F., Nicol, W. (2014) “Axial variation of wetting and liquid-solid mass transfer in long trickle bed columns”. *Industrial and Engineering Chemistry Research,* 53, 494–497.

Eisenburg, M., Tobais, C.W., Wilke, C.R. (1955) “Application of backside luggin capillaries in measurement of nonuniform polarization”. *Journal of Electrochemical Society,* 102(7), 415-419.

Gianetto, A., Baldi, G., Specchia, V., Sicardi, S. (1978) "Hydrodynamics and solid-liquid contact effectiveness in trickle bed reactors". *American Institute of Chemical Engineers Journal,* 24(6), 1087–1978.

Gostick, J., Doan, H.D., Lohi, A., Pritzker, M.D. (2003) “Investigation of local mass transfer in a packed bed of pall rings using a limiting current technique”. *Industrial and Engineering Chemical Research*, 42, 3626–3634.

Herskowitz, M., Smith, J.M. (1978) "Liquid distribution in tickle-bed reactors. Part I: Flow measurements". *American Institute of Chemical Engineers Journal,* 24(3), 439–450 .

Jolls, K.R., Hanratty, J.T. (1969) "Use of electrochemical techniques to study mass transfer rates and local skin friction to a sphere in a dump bed". *American Institute of Chemical Engineers Journal,* 15(2), 199–205.

Joubert, R., Nicol, W. (2009) “Multiplicity behaviour of trickle flow liquid-solid mass transfer”. *Industrial and Engineering Chemical Research*, 48, 8387–8392.

Joubert, R., Nicol, W. (2013) “Trickle flow liquid-solid mass transfer and wetting in smaller diameter columns”. *Canadian Journal of Chemical Engineering*, 91, 441–447.

Kan, K., Greenfield, P.F. (1983) “A residence-time model for trickle-flow reactors incorporating incomplete mixing in stagnant regions”. *American Institute of Chemical Engineers Journal*, 29(1), 123–132.

Kundu, A., Saroha, A.K., Nigam, K.D.P. (2001) “Liquid distribution studies in trickle-bed reactors”. *Chemical Engineering Science,* 56, 5963–5967.

Larachi, F., Grandjean, B. (1999) “tricklebed_flowsimulatordesign-1”. Available at: http://www.gch.ulaval.ca/

Levec, J., Grosser, K., Carbonall, R.G. (1988) “The hysteric behaviour of pressure drop and liquid hold-up in trickle bed reactors”. *American Institute of Chemical Engineers Journal*, 34(6), 1027–1030.

Loudon, D., Van der Merwe, W., Nicol, W. (2006) “Multiple hydrodynamic states in trickle flow: Quantifying the extent of pressure drop, liquid hold-up and gas-liquid mass transfer variations”. *Chemical Engineering Science,* 26, 7551–7562.

Maiti, R.N., Nigam, K.D.P. (2007) "Gas-liquid distributors for trickle bed reactors: A review" *Industrial Engineering Chemistry Research,* 46(19), 6164–6182.

Mitchell, J.E., Hanratty, J.T. (1966) "A study of turbulence at a wall using an electrochemical wall shear meter". *Journal Fluid Mechanics,* 26(1), 199–221.

Moccairo, C., Martinez, O.M., Barreto, G.F. (2013) “Assessment of mass transfer in the stagnate liquid region in trickle-bed reactors”. *Chemical Engineers Journal*, 173, 813-827.

Nicol, W., Joubert, R. (2013) "Liquid-solid mass transfer distributions in trickle bed reactors". *Chemical Engineering Journal*, 91(3), 361–366.

Rao, V.G., Drinkenburg, A.A.H. (1985) “Solid-liquid mass transfer in packed beds with co-current gas-liquid downflow”. *American Institute of Chemical Engineers Journal*, 31(7), 1059–1068.

Ravindra, P.V., Rao, D.P., Rao, S.M. (1997) “Liquid flow texture in trickle bed reactors: An experimental study”. *Industrial Engineering Chemistry Research,* 36, 5133-5145.

Reiss, L.P. (1967) “Cocurrent gas-liquid contacting in packed columns”. *I&EC Process Design and Development,* 6(4), 486-499.

Reiss, L.P., Hanratty, T.J. (1962) "Measurement of instantaneous rates of mass transfer to a small sink on a wall". *American Institute of Chemical Engineers Journal,* 8(2), 245–247.

Sederman, A.J., Gladden, L.F. (2001) “Magnetic resonance imaging as a quantitative probe of gas-liquid distribution and wetting efficiency in trickle-bed reactors”. *Chemical Engineering Science*, 56, 2615–2628.

Schubert, M., Hessel, G., Zippe, C., Lange, R., Hampel, U. (2008) “Liquid flow texture analysis in trickle bed reactors using high-resolution gamma ray tomography”. *Chemical Engineering Journal*,140, 332–340.

Sims, B.W., Schulz, F.G., Luss, D. (1993) "Solid-liquid mass transfer in a trickle bed". *Industrial Engineering Chemistry Research,* 32, 1895–1903.

Trivizadakis, M.E., Karabelas, A.J. (2006) “A study of local liquid/solid mass transfer in packed beds under trickling and induced pulsing flow”. *Chemical Engineering Science,* 61, 7684–7696.

Van der Merwe, W. (2008) “Trickle flow hydrodynamic multiplicity”. PhD thesis, Department of Chemical Engineering, University of Pretoria.

Van Houwelingen, A. (2006) “The morphology of solid-liquid contacting efficiency in trickle flow”. MSc dissertation, Department of Chemical Engineering, University of Pretoria.

Van Houwelingen, A., Sandrock, C., Nicol, W. (2006) “Particle wetting distribution in trickle bed reactors”. *Reactors, Kinetics and Catalysis*, 52(10), 3532–3542.

Vogtländer, P.H., Bakker, C.A.P. (1963) "An experimental study of mass transfer from a liquid flow to wires and gauze". *Chemical Engineering Science,* 18(9), 583–589.